J Therm Anal Calorim (2017) 127:2499–2509
DOI 10.1007/s10973-016-5871-2

Kinetic study of the CO_2 gasification of manure samples

M. Fernandez-Lopez[1] · D. López-González[2] · J. L. Valverde[1] · L. Sanchez-Silva[1]

Received: 6 May 2016 / Accepted: 18 September 2016 / Published online: 26 September 2016

Abstract The influence of the temperature on the gasification of two manure char samples (char Pre and char SW) was evaluated in a thermogravimetric analyser (TG) using CO_2 as the gasifying agent. Experimental data were fitted to seven kinetic models in order to reproduce accurately the gasification process. The classic volumetric (VM), shrinking core (SCM) and random pore (RPM) models were considered. In addition, four semi-empirical models based on them (SCM-Emp, RPM1, RPM2 and RPM3) were also tested. For the parameter estimation, a home-made VBA–Excel application was developed. The statistical meaningful of the models and their corresponding parameters were evaluated by using F and t tests, respectively. The best fittings were achieved with SCM (char Pre) and SCM-Emp (char SW) models. A catalytic promotion of the gasification process for char SW was observed, coming from the inorganic matter present in this sample. Consequently, the alkali index (A.I.) for both samples was calculated in order to check the catalytic behaviour of the metallic species contained in the corresponding ashes. As expected, the A.I. value corresponding to char SW was much higher than that of char Pre.

Keywords CO_2 gasification · Kinetics · Manure · TG

Introduction

In this century, the depletion of fossil fuel reserves has been associated with the growing energy demand which has caused, simultaneously, severe environmental problems, including air pollution, global warming and acid rain [1]. For this reason, renewable energies offer a good alternative to solve these drawbacks since they are a never-ending resource to human scale.

Renewable energies have many advantages such as the production of small amounts of wastes if compared to traditional energies. Moreover, the greenhouse gases (GHG) emission is minimal or zero [2, 3]. Nonetheless, some problems are associated with the use of the renewable energies: in the case of biomass transport over long distance need, difficulty of storing the excess of the produced energy and requirement of large spaces for growing them. Furthermore, its technology has not been totally established yet as the traditional sources of energy and more investigation is needed to improve and optimize the processes involved in order to make them economically viable.

Among the different renewable energy sources, biomass seems to be one of the most viable routes for the production of clean energy and chemical products. Biomass is defined as all kind of organic matter which could be used to produce energy [4]. Specifically, livestock biomass is generated from animal fats, carcasses and excrements, being this animal waste known as manure. Even though this type of biomass presents positive applications, its use has associated certain risks and dangers for environment and human healthy due to the presence of pathogens [5]. Moreover, traditional uses of livestock manure (LSM) have to be

Electronic supplementary material The online version of this article (doi:10.1007/s10973-016-5871-2) contains supplementary material, which is available to authorized users.

✉ L. Sanchez-Silva
marialuz.sanchez@uclm.es

[1] Department of Chemical Engineering, University of Castilla-La Mancha, Avda. Camilo José Cela 12, 13071 Ciudad Real, Spain

[2] Ircelyon, Institut de recherches sur la catalyse et l'environnement de Lyon, 2 Av. Albert Einstein, 69626 Lyon, France

changed due to land limitations and stricter regulations [6]. Therefore, the valorization of the manure surplus for bioenergy generation could be a sustainable choice since it is considered a zero-cost feedstock [7, 8].

Generally, the conversion of LSM into energy could be carried out through biological or thermochemical processes. One of the most common biological processes is the anaerobic digestion (AD), resulting in the generation of biogas and a residual digested. Concerning the thermochemical conversion routes, one of the main technologies to obtain syngas as well as fuel gas from biomass waste is the gasification process.

Compared to pyrolysis and combustion, there are few works reported in the literature about the gasification of biomass. Most works have been focused on the study of coals [9–12]. On the other hand, there are several studies focus on the evaluation of the conversion variation during the thermochemical processes. One of the most popular methods consists of measuring the gain or loss of mass while the reaction progresses, which is quite useful to verify if the sample decomposes or reacts with other components. In this regard, thermogravimetric analysis (TG) has been widely used for the kinetic study of the thermochemical conversion processes [13]. Specifically, the kinetic study of gasification is essential for modelling the gasification processes at industrial scale. Furthermore, the kinetic analysis of gasification has great importance for a correct design and product yield control [14].

Kinetic models usually describe the char reduction process using kinetic rate expressions obtained from experiments. In this regard, Scala studied the char gasification using both H_2O and CO_2 as the gasifying agent. Consequently, a kinetic model of the process was proposed based on experimental data [15].

Several biomass gasification models have been proposed in the literature. However, just three main models are commonly used: the volumetric model (VM), the grain or shrinking core model (SCM) and the random pore model (RPM). The complexity of the models can be reduced by making assumptions, but the levels of simplification have to be carefully evaluated to make them coherent with the final aim of the model [16]. In this regard, Xu et al. [17] studied the kinetic parameters of the CO_2 gasification of coal and biomass. They evaluated the above-mentioned models and calculated the kinetic parameters, concluding that RPM was the best model that fits the experimental results. Besides, Lahijani et al. [18] analysed the influence of alkali, alkaline earth and transition metal salts in the co-gasification of pistachio nut shell char, being its content in Na, an important factor in char gasification reactivity. They also concluded that the most suitable model to describe the reaction was RPM. Dupont et al. [19] analysed different models to find one that could predict the gasification reaction. They took into account the partial steam pressure and the influence of catalytic compounds by an integral parameter (αi). Finally, the best result was obtained with model RPM.

The aim of this study was to evaluate the gasification process of two different types of livestock manure char samples (a dairy and a swine ones) by means of TG. In addition, kinetic analysis of the gasification process at different gasification temperatures was carried out. For this purpose, seven phenomenological models were evaluated: VM, SCM, SCM-Empirical (SCM-Emp), RPM and three variations of RPM.

Materials and methods

Biomass char samples preparation

The manure samples used in this study were two animal waste obtained from the province of Quebec (Canada): dairy (Pre) and swine (SW). Char samples (char Pre and char SW) were obtained by pyrolysing 10 grams of the manure samples in a tubular reactor. The devolatilization of the samples took placed from room temperature to 980 °C using a heating rate of 10 °C min^{-1} and a continuous He flow of 200 N mL min^{-1}. The samples were kept at 980 °C for 1 h, and the He flow was maintained until the drop of the temperature to ambient one to prevent reaction with air. Once both char samples were obtained, they were sieved to an average particle size of 50–100 μm.

Characterization of manure biomass samples

Both manure samples were characterized by elemental analysis, thermogravimetric analysis (TG) and atomic emission spectroscopy inductively coupled plasma (ICP-AES).

The ultimate analysis was used to measure the carbon (C), hydrogen (H), nitrogen (N), oxygen (O) and sulphur (S) content in the sample, following the standard UNE-EN 15104:2011. The equipment was capable of detecting all elements cited by various mechanisms; the result was given in mass percentage of each element in dry basis.

The proximate analysis was used to determine the four more relevant chemical characteristics of any type of fuel: moisture, ash, fixed carbon and volatile matter content. The equipment used to perform the proximate analysis was a thermogravimetric analyzer (TGA/DSC Model 1 METTLER TOLEDO STAR^e System) according to standard ASTM D 3172-73(84).

Finally, A VARIAN LIBERTY RL sequential ICP-AES elemental analysis was used to obtain the mass percentage of metallic elements present in the manure samples.

Table 1 Ultimate and proximate analyses and mineral content of samples char Pre and char SW

Samples	Ultimate analysis/mass%[a]					Proximate analysis/mass%			
	C	H	N	S	O^{diff}	Moisture	Ash	Volatile matter	Fixed carbon^{diff}
Pre char	40.19	0.57	0.22	0.16	2.01	2.85	56.85	10.33	33.55
SW char	60.50	0.70	1.00	0.52	3.86	2.12	33.42	10.75	55.83
	Mineral content/ppm								
	Al	Ca	Fe	Mg	Na	Ni	P	Si	
Pre char	5864	28,322	8696	9744	11,377	–	25,818	9961	
SW char	1097	25,015	6489	9873	5380	–	22,715	6280	

[a] *daf* dry ash free, O^{diff} obtained by difference of C, H, N, S and ash; *Fixed carbon*^{diff} calculated from the difference of moisture, ash and volatile matter

Table 1 shows the proximate and ultimate analyses and the mineral content of the studied char samples.

Gasification experiments: TG analysis

The gasification of samples char Pre and char SW were carried out using a TG apparatus (TGA-DSC 1, METTLER TOLEDO) operating at atmospheric pressure. Sample mass was fixed at 7 mg, and the particle size was kept in the 50–100 μm range. Firstly, a heating of the pyrolysed sample was performed at 40 °C min^{-1} under an inert gas to reach the gasification temperature. Once the gasification temperature was reached, the corresponding vol% of gasifying agent (CO_2) was injected into the Ar flow (before entering to the furnace) for 60 min until the end of the gasification process. 15 vol% CO_2 was used because it is the typical concentration of an effluent stream coming from anaerobic digestions or a flue gas coming from any combustion or gasification plants [20, 21]. The experimental errors in the determination of both the mass loss and the measure of the temperature were ±0.5 % and ±2 °C, respectively.

Char reactivity

The more extended definition to evaluate the char reactivity is based on the definition of the overall rate (R_i) as follows (Eq. 2.1) [22–25]:

$$R_i = -\frac{1}{w_i}\cdot\frac{dw_i}{dt} = \frac{1}{1-x_i}\cdot\frac{dx_i}{dt} \quad (2.1)$$

where x_i and w_i are the conversion and mass of char at any time, respectively, being the conversion x defined as follows:

$$x = \frac{m_0 - m_t}{m_0 - m_f} \quad (2.2)$$

where m_0, m_t and m_f represents the mass at time $t = 0$, $t = t$ and $t = t_f$, being t_f the final time of the process, respectively.

The reactivity is a function of the temperature and the gas composition, varying with the conversion degree [23, 26]. Therefore, a representative value of the reactivity was needed in order to make reliable comparisons. In this work, the reactivity at 50 % of char conversion was considered to be representative (R_{50}) [22, 25, 26].

The gasification rate (r_i) was also used to describe the gasification reaction and was calculated by Eq. 2.3 [27]:

$$r_i = \frac{dx_i}{dt} \quad (2.3)$$

Kinetic models

Thermogravimetric experiments were carried out with an isothermal temperature programme. Mass loss was measured as a function of the time. The rate of the process (dx/dt) can be parameterized as a function of the temperature, T, the extent of conversion, x, and the pressure, P as follows:

$$\frac{dx}{dt} = k(T)f(x)h(P) \quad (2.4)$$

The pressure dependence $h(P)$ is ignored in most of the kinetics studies reported [28]. Therefore, the rate is considered to be as a function of the temperature, T, and the extent of conversion, x:

$$\frac{dx}{dt} = k(T)f(x) \quad (2.5)$$

Equation (2.5) represents the reaction rate of a single-step process. Although the process mechanism involves more than one reaction, one of them could determine the overall

kinetics [28]. Therefore, Eq. (2.5) can be used to describe the overall reaction rate of the thermochemical processes.

The temperature dependence $k(T)$ is typically parameterized by the Arrhenius equation:

$$k(T) = Ae^{\frac{-E_a}{RT}} \tag{2.6}$$

where A is the preexponential factor, E_a the activation energy and R the universal gas constant. These kinetic parameters, which are experimentally determined, are called "effective" or "apparent" parameters because they represent the overall process and not the individual parameters of each step or reaction. In following sections, the word "apparent" will be omitted, but the activation energy will always be referred to as the apparent activation energy.

According to the literature [29–31], the volumetric model (VM), the shrinking core model (SCM) and the random pore model (RPM) are the three most popular models used to define $f(x)$. These models are based on phenomenological aspects of the gasification process by taking into account different assumptions. Volumetric model (VM) assumes a homogeneous reaction throughout the particle and a linear decrease in the reaction surface area with conversion [29]. On the other hand, shrinking core model (SCM) and random pore model (RPM) describe the evolution of the solid structure with the conversion. SCM assumes that a porous particle consists of an assembly of uniform nonporous grains and the reaction takes places on the surface of the grains assuming a spherical shape of the porous. RPM considers the overlapping of pore surfaces, reducing the available area for the reaction [14].

However, these models usually fail in the prediction of the well-known catalytic effect of ashes [14]. Therefore, some authors proposed some variation of them [1, 14, 18] by the addition of new terms to the parent models in order to predict the catalytic activity of the inorganic matter at high conversion values. In this regard, four additional models were proposed in this work, three of them derived from RPM, namely RPM1, RPM2, RPM3 and a semi-empirical SCM, namely SCM-Emp. Table 2 summarizes the mathematical expressions of the seven models proposed to fit the gasification experimental data.

For the parameter calculation, a home-made VBA–Excel application was developed to solve these models. The Runge–Kutta–Ferhlberg was used in the evaluation of the ordinary differential equation set, whereas the Levenberg–Marquardt algorithm was used in the nonlinear regression procedure [32].

The weighted sum of the squared differences between the experimental data (Exp) and the calculated data (Fit) degree of conversion was minimized according to the following equation:

Table 2 Gasification models and their mathematical expressions

Model	Mathematical expression
VM	$f(x) = (1-x)$
SCM	$f(x) = (1-x)^{2/3}$
SCM-Emp	$f(x) = (1-x)^{2/3} + K_a \cdot x^{n_a}$
RPM	$f(x) = (1-x) \cdot \sqrt{1 - \Psi \cdot \ln(1-x)}$
RPM1	$f(x) = (1-x)\sqrt{1 - \Psi \cdot \ln(1-x)} + K_a$
RPM2	$f(x) = (1-x) \cdot \sqrt{1 - \Psi \cdot \ln(1-x)} + K_a \cdot x$
RPM3	$f(x) = (1-x) \cdot \sqrt{1 - \Psi \cdot \ln(1-x)} + K_a \cdot x^{n_a}$

x = degree of conversion; Ψ = parameter related to the initial pore structure of the sample (at $x = 0$); K_a = the catalytic activation constant and n_a = the catalytic activation order

$$\chi^2 = \sum_{i=0}^{n}\sum_{j=0}^{m} \frac{\left(x_{i\,Fit} - x_{i\,Exp}\right)^2}{x_{i\,Exp}} \tag{2.7}$$

where i represents the number of equations to be fitted, j is the specific experimental data and n and m are the total number of equations and experimental data, respectively. Furthermore, the estimated parameters were statistically evaluated by the F and t tests.

F test is a test which has an F distribution under the null hypothesis. The procedure consists of the comparison between the tabulated F value (F test) and F_{mq} which are described elsewhere [33]. If F_{mq} is larger than the corresponding F test, assuming a value of $\alpha = 0.05$, 95 % confidence level, the regression was considered to be meaningful. On the other hand, the meaningfulness of each parameter in the model must be also evaluated.

t Test considers that the statistical hypothesis test follows a t Student distribution and allows to verify if the estimation of the parameter differs from a reference value (generally zero). It means that the t_{mq} value must be larger than t test value for each parameter as described elsewhere [33]. Therefore, if both the F test and the t test are met, the model and its parameters are statistically suitable for modelling the manure gasification process.

Finally, to ensure the goodness of the models, the mean error (%) obtained between the theoretical values (values given by the proposed model) and the experimental was calculated as follows:

$$\text{Mean error}\,(\%) = \sum_{j=0}^{M} \frac{\left(x_{j\,Fit} - x_{j\,Exp}\right)^2}{M} \tag{2.8}$$

where j represents the specific experimental data and M the total number of experimental data.

Results and discussion

Influence of gasification temperature

The process of gasification of biomass is mainly dependent on the biomass type and the operating conditions [34]. Particle size, char porosity, char mineral content, temperature and partial pressure of the gasifying agent are main physical factors that influence on the gasification rates [35]. In this work, the effect of temperature of the gasification process of two different manure samples (char Pre and char SW) was evaluated. CO_2 was selected as the gasifying agent, and its partial pressure was kept constant at 15 vol% during all the process.

Figure 1 shows the thermogravimetric (TG) profile of the gasification process for samples char Pre (Fig. 1a) and char SW (Fig. 1b) at 800, 850 and 900 °C. It can be seen from Fig. 1 that the gasification process started as soon as the gasifying agent (CO_2) reached the surface of the sample. In Fig. 1b, the TG profile of the char SW gasification at 800 °C shows that the sample was not totally gasified after 60 min of time on stream. Concerning the amount of final residue that remained after the gasification process, there were no significant differences among them at the three tested temperatures.

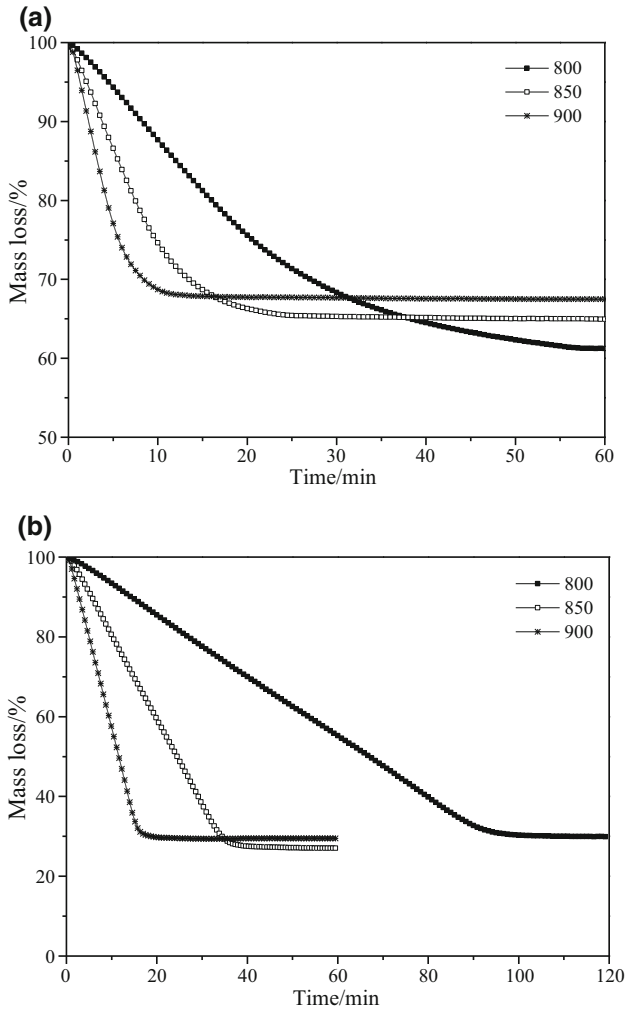

Fig. 1 Thermogravimetric profiles of CO_2 gasification process for samples: **a** char Pre and **b** char SW at 800, 850 and 900 °C

Reactivity at 50 % of char conversion (R_{50}) and times to reach 50 and 99 % of char conversion (x_{50} and x_{99}, respectively) are summarized in Table 3 for samples char Pre and char SW. These parameters allowed to establish a comparison between the behaviour of both samples during the gasification process. As it is well known, the gasification is an endothermic process that is favoured at high temperatures. Figure 2 shows the conversion values versus time on stream for samples char Pre and char SW at 800, 850 and 900 °C. In the case of sample char SW, it was not possible to finish the gasification process at 800 °C during a moderated time span. Therefore, the gasification time for these samples was of 120 min instead of 60 min. As observed in Table 3 and Fig. 2, the higher the temperature, the higher the reactivity of both samples was. As the reactivity of the samples depends on the sample chemical structure, the porosity and the inorganic constituents [23], nitrogen adsorption/desorption isotherms were performed to evaluate the influence of the char structure on the reactivity. Table 4 shows the BET surface area and the micropore volume for all the samples studied. It can be observed that sample char Pre presented the higher surface area. Consequently, its gasification proceeded at higher rates [36]. The effect of the temperature and the char structure were also observed when the reactivity and the gasification rate at 800, 850 and 900 °C were plotted against conversion (Fig. 3). It can be observed in Fig. 3 that both the reactivity and the gasification rate increased with the temperature. Regarding the gasification rate, sample char Pre showed the highest values which are consistent with its values of surface area. However, at low conversion values, the reactivity was higher for sample char Pre although this trend changed at higher conversion values. As noticed, the reactivity values of char SW increased suddenly at $X \geq 0.85$. This fact can be attributed to the presence of indigenous inorganic matter in the biomass composition which is catalytic in nature [37]. As the gasification process proceeded, the carbon material was consumed and the metal-to-carbon ratio increased, which strengthened the catalytic effect as more active sites were available [14]. The different shapes of the TG gasification profiles confirmed the catalytic effect of the inorganic matter contained in the parent sample char SW [36, 38, 39].

In this regard, numerical indexes such as the alkali index (A.I.) proposed by Sakawa et al. have been defined to

Table 3 Gasification parameters for samples char Pre and char SW at 800, 850 and 900 °C

Gasification temperature	Char Pre			Char SW		
	Time x_{99}/min	Time x_{50}/min	R_{50}/min^{-1}	Time x_{99}/min	Time x_{50}/min	R_{50}/min^{-1}
800 °C	54.50	15.57	0.06	97.05	46.77	0.02
850 °C	29.30	6.57	0.15	38.42	18.07	0.06
900 °C	16.87	3.52	0.31	18.05	8.38	0.13

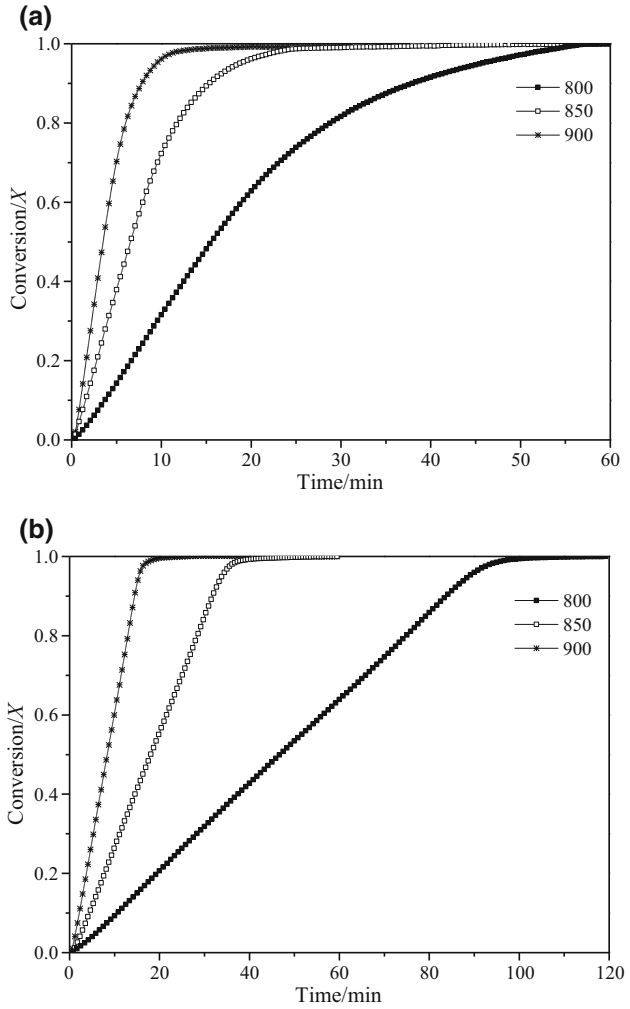

Fig. 2 Conversion profiles versus time: **a** sample char Pre and **b** sample char SW at different gasification temperatures

describe the catalytic efficiency of active species within the ash [14, 40–43]. The A.I. is calculated as the ratio of the fraction sum of the basic compounds with catalytic nature in the ash to the fraction of the acidic compounds with non-catalytic nature as follows:

Table 4 Surface area and micropore volume for the samples char Pre and char SW

Biomass sample	Surface area/m^2 g^{-1}	Micropore volume[a]/cm^3 g^{-1}
Char Pre	35.6	0.00263
Char SW	8.2	0.00066

[a] Cumulative micropore volume obtained using the Horvath–Kowazoe method

$$\text{A.I.} = \frac{\text{Ash}\,(\text{mass}\%)}{100} \cdot \frac{(\text{CaO} + \text{K}_2\text{O} + \text{MgO} + \text{Na}_2\text{O} + \text{Fe}_2\text{O}_3)(\text{mass}\%)}{(\text{Al}_2\text{O}_3 + \text{SiO}_2)(\text{mass}\%)} \quad (2.9)$$

Therefore, A.I. was 1.65 and 1.72 for samples char Pre and char SW, respectively. Although the highest amount of ash and mineral content was associated with sample char Pre (Table 1), the value A.I. was higher for sample char SW which would explain the higher reactivity of this sample at higher conversion values.

Gasification kinetic analyses

Once the effect of temperature was evaluated, the kinetic analysis of the gasification process of the two biomass manure samples here tested was performed. This analysis supposes the first step for the industrial process modelling. Furthermore, knowledge of the kinetics is important for a correct design and product yield control [44].

Figures 4 and 5 show the quality of the fitting of the different models here considered to the experimental data of the gasification process at 800, 850 and 900 °C for samples char Pre and char SW, respectively. Tables SS1–SS6 summarize the obtained gasification parameters and the statistical significance of each model for samples char Pre and char SW at different gasification temperatures.

In this work, the goodness of a model has been evaluated by means of the error obtained between the theoretical

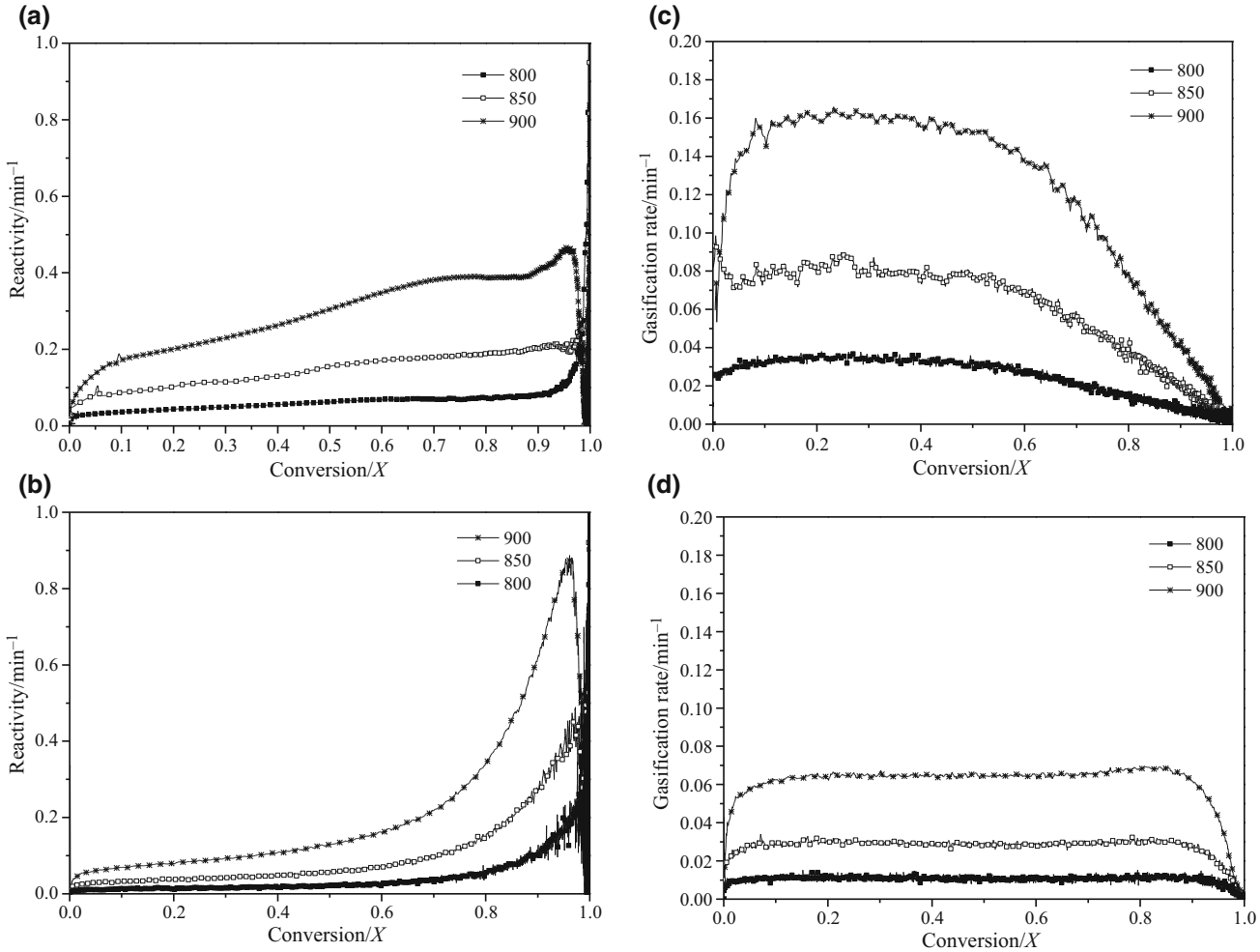

Fig. 3 Reactivity (**a**, **b**) and gasification rate (**c**, **d**) versus conversion profiles of samples char Pre and char SW at 800, 850 and 900 °C

values (values given by the proposed model) and the experimental ones, as well as by the corresponding value of χ^2. In this regard, the lower the error and χ^2 values, the better the fitting was.

It can be observed from Figs. 4 and 5 that the shrinking core model (SCM) achieved the best fitting to the experimental curves for sample char Pre, whereas the rest models obtained high mean errors, meaning that the value of χ^2 was found to be high. However, for the gasification experiment at 800 °C, the best model that fitted the experimental data was the semi-empirical shrinking core one (SCM-Emp). This model was used by López-González et al. [14] in their experiments to predict the experimental data of lignocellulosic biomass samples gasification. The better fitting of this semi-empirical model was ascribed to its capacity of predicting the catalytic activity of the ashes at high conversions by the addition of a potential term. The catalytic activity of the ashes was more noticeable at high conversions since the ratio catalyst/biomass increased along time. Thus, the contribution of a potential term was higher at high conversion, whereas at low conversions it can be considered negligible. Nevertheless, the statistical significance of these parameters was not higher enough to confirm that the catalytic matter had a substantial influence on the gasification process; i.e. the catalytic effect was not strong.

On the other hand, the best model which fitted the experimental data obtained with sample char SW was the semi-empirical shrinking core one (SCM-Emp), pointing out that the catalytic activity of the inorganic matter during the gasification of this sample was more pronounced and significant than that observed in the gasification of sample char Pre.

Concerning the effect of the gasification temperature on the kinetic parameters, the higher the temperature, the higher the kinetic constant k for both samples. Moreover, in the case of sample char SW, an additional catalytic constant rate was considered (k_a). However, the same trend with temperature was observed for constant k_a. Tables 5

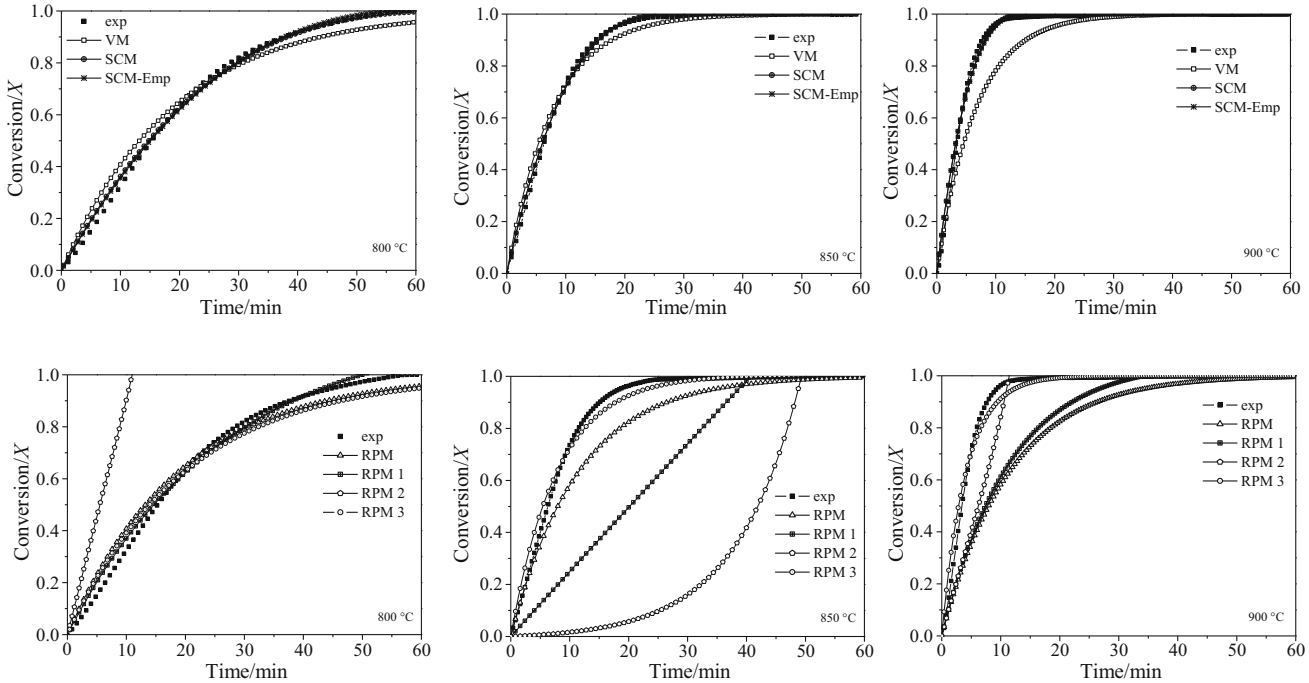

Fig. 4 Prediction of the proposed models for the gasification of sample char Pre at 800, 850 and 900 °C

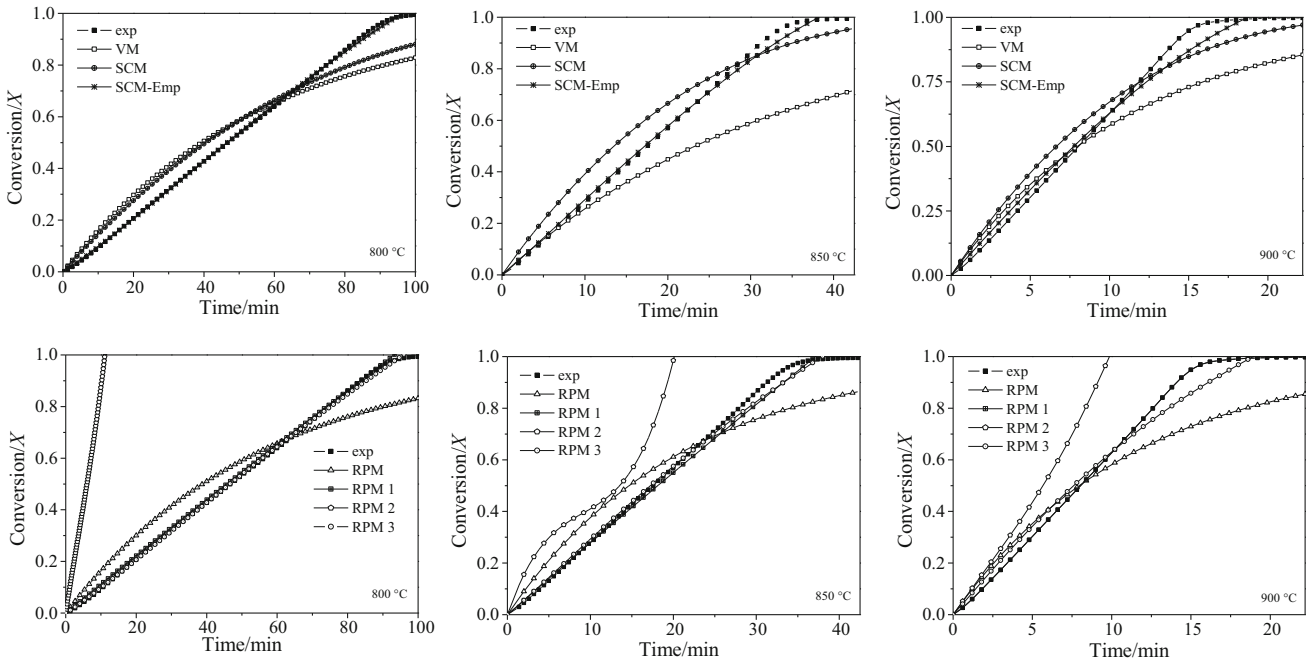

Fig. 5 Prediction of the proposed models for the gasification of sample char SW at 800, 850 and 900 °C

and 6 show for samples char Pre and char SW, respectively, the estimated kinetic parameters obtained with the best fitting model.

In addition, the Arrhenius plot ($\ln(k)$ vs $1/T$) is shown in Fig. 6 for samples char Pre and char SW. The k values used were selected from the best model which fitted the experimental data at each gasification temperature. The gasification temperatures evaluated in this study were under 1000 °C, which is generally considered a low temperature for a gasification process [18]. Therefore, the char gasification under the experimental conditions used should have been performed under the chemically controlled reaction regime [35]. According to this Arrhenius plot, the activation energy values for the CO_2 gasification process of samples

Table 5 Best fitting model and its parameter values for sample char Pre at each gasification temperature

Gasification temperature	Model	Parameters	Value	± Error
800 °C	SCM-Emp	k	0.0397	5.40E−04
		K_a	0.0016	3.44E−04
		n_a	0.3021	3.35E−02
850 °C	SCM	k	0.1029	6.10E−04
900 °C	SCM	k	0.1939	1.94E−03

Table 6 Best fitting model and its parameter values for sample char SW at each gasification temperature

Gasification temperature	Model	Parameters	Value	± Error
800 °C	SCM-Emp	k	0.0069	1.26E−05
		K_a	0.0082	5.93E−05
		n_a	0.3077	6.17E−03
850 °C	SCM-Emp	k	0.0254	1.18E−03
		K_a	0.0168	3.35E−04
		n_a	0.4724	6.88E−02
900 °C	SCM-Emp	k	0.0690	1.54E−03
		K_a	0.0270	6.33E−05
		n_a	0.8780	9.73E−03

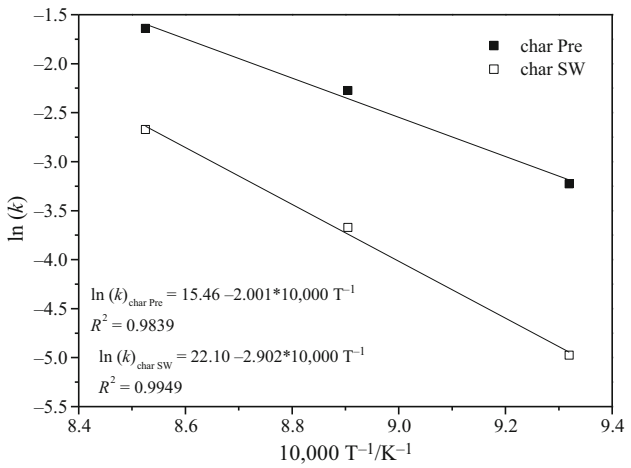

Fig. 6 Arrhenius plots for samples char Pre and char SW at different gasification temperatures

char Pre and char SW were 166.4 and 241.3 kJ mol^{-1}, respectively.

Conclusions

In this work, the kinetic analysis of the CO_2 gasification process of two manure char samples was performed. The temperature had a direct influence on the CO_2 gasification process of manure char samples The gasification rate and reactivity parameters were also calculated to corroborate this effect.

The values of reactivity, gasification rate and time to achieve total conversion confirmed the temperature influence on the gasification process. The lower values were found at 800 °C, whereas the higher ones were obtained at 900 °C. Moreover, it can be observed that sample char SW required more time to be totally gasified during the experiment at 800 °C.

Furthermore, the alkali index (A.I.) was calculated, being 1.65 and 1.72 for samples char Pre and char SW, respectively. The higher value was found for sample char SW, which would be explained its higher reactivity at higher conversion values.

The best models to fit the gasification process of samples char Pre and char SW were SCM and the SCM-Emp ones, respectively. Although the best model for predicting the gasification of sample of char Pre at 800 °C was the SCM-Emp, the statistical significance of the catalytic parameters was not high enough. Moreover, the differences of fitting between models SCM-Emp and SCM were quite low, indicating that the catalytic effect was not pronounced.

Acknowledgements Authors acknowledge the financial support from the Regional Government of Castilla-La Mancha (Project PEII-2014-007-P) and also from the University of Castilla-La Mancha of Spain (UCLM grant). The authors also thank to the *Institut de recherches sur la catalyse et l'environnement* of Lyon and the *Centre National en Électrochimie et en Technologies Environnementales (CNETE)* for its in-kind contribution.

References

1. Ding L, Zhang Y, Wang Z, Huang J, Fang Y. Interaction and its induced inhibiting or synergistic effects during co-gasification of coal char and biomass char. Bioresour Technol. 2014;173:11–20. doi:10.1016/j.biortech.2014.09.007.
2. Cherubini F, Strømman AH. Life cycle assessment of bioenergy systems: state of the art and future challenges. Bioresour Technol. 2011;102(2):437–51. doi:10.1016/j.biortech.2010.08.010.
3. Zanatta ER, Reinehr TO, Awadallak JA, Kleinübing SJ, dos Santos JBO, Bariccatti RA, et al. Kinetic studies of thermal decomposition of sugarcane bagasse and cassava bagasse. J Therm Anal Calorim. 2016;125(1):437–45. doi:10.1007/s10973-016-5378-x.
4. Van Dael M, Van Passel S, Pelkmans L, Guisson R, Reumermann P, Luzardo NM, et al. A techno-economic evaluation of a biomass energy conversion park. Appl Energy. 2013;104:611–22. doi:10.1016/j.apenergy.2012.11.071.
5. Nicholson FA, Groves SJ, Chambers BJ. Pathogen survival during livestock manure storage and following land application. Bioresour Technol. 2005;96(2):135–43. doi:10.1016/j.biortech.2004.02.030.
6. Sharara MA, Sadaka SS, Costello TA, VanDevender K, Carrier J, Popp M, et al. Combustion kinetics of swine manure and algal solids. J Therm Anal Calorim. 2016;123(1):687–96. doi:10.1007/s10973-015-4970-9.
7. Otero M, Sánchez ME, Gómez X. Co-firing of coal and manure biomass: a TG–MS approach. Bioresour Technol. 2011;102(17):8304–9. doi:10.1016/j.biortech.2011.06.040.
8. Otero M, Sanchez ME, Gómez X, Morán A. Thermogravimetric analysis of biowastes during combustion. Waste Manag (Oxford). 2010;30(7):1183–7. doi:10.1016/j.wasman.2009.12.010.
9. Shabbar S, Janajreh I. Thermodynamic equilibrium analysis of coal gasification using Gibbs energy minimization method. Energy Convers Manag. 2013;65:755–63.
10. Tay HL, Kajitani S, Zhang S, Li CZ. Effects of gasifying agent on the evolution of char structure during the gasification of Victorian brown coal. Fuel. 2013;103:22–8.
11. Umemoto S, Kajitani S, Hara S. Modeling of coal char gasification in coexistence of CO_2 and H_2O considering sharing of active sites. Fuel. 2013;103:14–21.
12. Liu L, Liu Q, Cao Y, Pan W-P. The isothermal studies of char-CO_2 gasification using the high-pressure thermo-gravimetric method. J Therm Anal Calorim. 2015;120(3):1877–82. doi:10.1007/s10973-015-4476-5.
13. Kozlov A, Svishchev D, Donskoy I, Shamansky V. Impact of gas-phase chemistry on the composition of biomass pyrolysis products. J Therm Anal Calorim. 2015;122(3):1089–98. doi:10.1007/s10973-015-4951-z.
14. López-González D, Fernandez-Lopez M, Valverde JL, Sanchez-Silva L. Gasification of lignocellulosic biomass char obtained from pyrolysis: kinetic and evolved gas analyses. Energy. 2014;71:456–67. doi:10.1016/j.energy.2014.04.105.
15. Scala F. Fluidized bed gasification of lignite char with CO_2 and H_2O: a kinetic study. Proc Combust Inst. 2015;35(3):2839–46. doi:10.1016/j.proci.2014.07.009.
16. Ranzi E, Dente M, Goldaniga A, Bozzano G, Faravelli T. Lumping procedures in detailed kinetic modeling of gasification, pyrolysis, partial oxidation and combustion of hydrocarbon mixtures. Prog Energy Combust. 2001;27(1):99–139. doi:10.1016/s0360-1285(00)00013-7.
17. Xu C, Hu S, Xiang J, Yang H, Sun L, Su S, et al. Kinetic models comparison for steam gasification of coal/biomass blend chars. Bioresour Technol. 2014;171(1):253–9. doi:10.1016/j.biortech.2014.07.099.
18. Lahijani P, Zainal ZA, Mohamed AR, Mohammadi M. CO_2 gasification reactivity of biomass char: catalytic influence of alkali, alkaline earth and transition metal salts. Bioresour Technol. 2013;144:288–95. doi:10.1016/j.biortech.2013.06.059.
19. Dupont C, Nocquet T, Da Costa JA, Verne-Tournon C. Kinetic modelling of steam gasification of various woody biomass chars: influence of inorganic elements. Bioresour Technol. 2011;102(20):9743–8.
20. Irfan MF, Usman MR, Kusakabe K. Coal gasification in CO_2 atmosphere and its kinetics since 1948: a brief review. Energy. 2011;36(1):12–40. doi:10.1016/j.energy.2010.10.034.
21. Guizani C, Escudero Sanz FJ, Salvador S. The gasification reactivity of high-heating-rate chars in single and mixed atmospheres of H_2O and CO_2. Fuel. 2013;108:812–23. doi:10.1016/j.fuel.2013.02.027.
22. Mandapati RN, Daggupati S, Mahajani SM, Aghalayam P, Sapru RK, Sharma RK, et al. Experiments and kinetic modeling for CO_2 gasification of Indian coal chars in the context of underground coal gasification. Ind Eng Chem Res. 2012;51(46):15041–52.
23. Di Blasi C. Combustion and gasification rates of lignocellulosic chars. Prog Energy Combust Sci. 2009;35(2):121–40. doi:10.1016/j.pecs.2008.08.001.
24. Fermoso J, Arias B, Pevida C, Plaza MG, Rubiera F, Pis JJ. Kinetic models comparison for steam gasification of different nature fuel chars. J Therm Anal Calorim. 2008;91(3):779–86.
25. Zhang L, Huang J, Fang Y, Wang Y. Gasification reactivity and kinetics of typical Chinese anthracite chars with steam and CO_2. Energy Fuels. 2006;20(3):1201–10.
26. Gómez-Barea A, Ollero P, Fernández-Baco C. Diffusional effects in CO_2 gasification experiments with single biomass char particles. 1. Experimental investigation. Energy Fuels. 2006;20(5):2202–10.
27. Huang Y, Yin X, Wu C, Wang C, Xie J, Zhou Z, et al. Effects of metal catalysts on CO_2 gasification reactivity of biomass char. Biotechnol Adv. 2009;27(5):568–72.
28. Vyazovkin S, Burnham AK, Criado JM, Pérez-Maqueda LA, Popescu C, Sbirrazzuoli N. ICTAC Kinetics Committee recommendations for performing kinetic computations on thermal analysis data. Thermochim Acta. 2011;520(1–2):1–19. doi:10.1016/j.tca.2011.03.034.
29. H-b Zuo, W-w Geng, J-l Zhang, G-w Wang. Comparison of kinetic models for isothermal CO_2 gasification of coal char-biomass char blended char. Int J Miner Met Mater. 2015;22(4):363–70. doi:10.1007/s12613-015-1081-3.
30. Sircar I, Sane A, Wang W, Gore JP. Experimental and modeling study of pinewood char gasification with CO_2. Fuel. 2014;119:38–46. doi:10.1016/j.fuel.2013.11.026.
31. Gil MV, Riaza J, Álvarez L, Pevida C, Pis JJ, Rubiera F. Kinetic models for the oxy-fuel combustion of coal and coal/biomass blend chars obtained in N_2 and CO_2 atmospheres. Energy. 2012;48(1):510–8. doi:10.1016/j.energy.2012.10.033.
32. Press WH. Numerical recipes 3rd edition: the art of scientific computing. Cambridge: Cambridge University Press; 2007.
33. De La Osa AR, De Lucas A, Romero A, Valverde JL, Sánchez P. Kinetic models discrimination for the high pressure WGS reaction over a commercial CoMo catalyst. Int J Hydrogen Energy. 2011;36(16):9673–84.
34. Naidu VS, Aghalayam P, Jayanti S. Evaluation of CO_2 gasification kinetics for low-rank Indian coals and biomass fuels. J Therm Anal Calorim. 2016;123(1):467–78. doi:10.1007/s10973-015-4930-4.
35. Mani T, Mahinpey N, Murugan P. Reaction kinetics and mass transfer studies of biomass char gasification with CO_2. Chem Eng Sci. 2011;66(1):36–41.

36. Duman G, Uddin MA, Yanik J. The effect of char properties on gasification reactivity. Fuel Process Technol. 2014;118:75–81. doi:10.1016/j.fuproc.2013.08.006.
37. Lv D, Xu M, Liu X, Zhan Z, Li Z, Yao H. Effect of cellulose, lignin, alkali and alkaline earth metallic species on biomass pyrolysis and gasification. Fuel Process Technol. 2010;91(8):903–9. doi:10.1016/j.fuproc.2009.09.014.
38. Struis RPWJ, Von Scala C, Stucki S, Prins R. Gasification reactivity of charcoal with CO_2. Part I: conversion and structural phenomena. Chem Eng Sci. 2002;57(17):3581–92.
39. Struis RPWJ, Von Scala C, Stucki S, Prins R. Gasification reactivity of charcoal with CO_2. Part II: metal catalysis as a function of conversion. Chem Eng Sci. 2002;57(17):3593–602.
40. Li J, Zhu M, Zhang Z, Zhang D. A new criterion for determination of coal ash sintering temperature using the pressure-drop technique and the effect of ash mineralogy and geochemistry. Fuel. 2016;179:71–8. doi:10.1016/j.fuel.2016.03.078.
41. Sakawa M, Sakurai Y, Hara Y. Influence of coal characteristics on CO_2 gasification. Fuel. 1982;61(8):717–20.
42. Wang Y-L, Zhu S-H, Gao M-Q, Yang Z-R, Yan L-J, Bai Y-H, et al. A study of char gasification in H_2O and CO_2 mixtures: role of inherent minerals in the coal. Fuel Process Technol. 2016;141(Part 1):9–15. doi:10.1016/j.fuproc.2015.06.001.
43. Hattingh BB, Everson RC, Neomagus HWJP, Bunt JR. Assessing the catalytic effect of coal ash constituents on the CO_2 gasification rate of high ash, South African coal. Fuel Process Technol. 2011;92(10):2048–54. doi:10.1016/j.fuproc.2011.06.003.
44. Cordero T, Rodríguez-Maroto JM, Rodríguez-Mirasol J, Rodríguez JJ. On the kinetics of thermal decomposition of wood and wood components. Thermochim Acta. 1990;164(C):135–44.